

## Extracting the resonance parameters from experimental data on scattering of charged particles

P. Vaandrager\* and S. A. Rakityansky†

*Department of Physics, University of Pretoria,  
Lynnwood Road, Pretoria, 0002, South Africa*

*\*paul.vaandrager@up.ac.za*

*†rakitsa@up.ac.za*

Received 1 December 2015

Accepted 3 January 2016

Published 17 February 2016

A new parametrization of the multi-channel  $S$ -matrix is used to fit scattering data and then to locate the resonances as its poles. The  $S$ -matrix is written in terms of the corresponding “in” and “out” Jost matrices which are expanded in the Taylor series of the collision energy  $E$  around an appropriately chosen energy  $E_0$ . In order to do this, the Jost matrices are written in a semi-analytic form where all the factors (involving the channel momenta and Sommerfeld parameters) responsible for their “bad behavior” (i.e., responsible for the multi-valuedness of the Jost matrices and for branching of the Riemann surface of the energy) are given explicitly. The remaining unknown factors in the Jost matrices are analytic and single-valued functions of the variable  $E$  and are defined on a simple energy plane. The expansion is done for these analytic functions and the expansion coefficients are used as the fitting parameters. The method is tested on a two-channel model, using a set of artificially generated data points with typical error bars and a typical random noise in the positions of the points.

*Keywords:* Jost matrix; multi-channel resonances; energy Riemann surface; Coulomb forces.

PACS Number(s): 03.65.Nk, 24.10.Eq, 29.85.Fj, 24.10.-i, 24.30.-v

### 1. Introduction

The main parameters that characterize any quantum resonance are the collision energy  $E_r$ , at which this state can be excited and the width  $\Gamma$  that determines the lifetime of the state. For a multi-channel system the total width is the sum of the partial widths,  $\Gamma = \Gamma_1 + \Gamma_2 + \dots$ , where  $\Gamma_n/\Gamma$  gives the relative probability of decaying into the  $n$ th channel. There are many different methods for determining these parameters from a set of scattering data (several of them are described in Refs. 1, 2). These methods form two big groups based on two principally different approaches.

Within the first approach, the parameters  $E_r$ ,  $\Gamma$ ,  $\Gamma_1$ ,  $\Gamma_2$ , etc. are treated as the adjustable variables in a procedure of fitting the available experimental data. The simplest and most well-known example of such a method is the Breit–Wigner parametrization of the amplitude.<sup>3</sup> A common feature of all of the methods belonging to this category is that the number of resonances is fixed from the outset. All these methods use some parametric expression for the amplitude, or for the  $S$ -matrix, or directly for the cross-section, where the resonance singularities (or the zigzags of the cross-section) are embedded into this parametric expression by hand. These methods only differ in the method of parametrization and in the derivation of the parametric expression.

Within the second approach, the resonances are considered as the poles of the  $S$ -matrix at the complex energies  $E_r - i\Gamma/2$  in an appropriate domain of the Riemann surface of the energy. The  $S$ -matrix is written in a more general form with some adjustable parameters that do not necessarily coincide with the resonance parameters. Usually, it is not known beforehand how many resonances can be found (if any). After fitting the data at real collision energies, the analytic expression for the  $S$ -matrix thus obtained is examined at complex energies where the poles (if found) are interpreted as the resonances. The Padé approximation of the  $S$ -matrix<sup>1,4,5</sup> and the Laurent–Pietarinen series expansion of the amplitude<sup>6</sup> can be mentioned as examples.

The method we describe here belongs to the second category and is based on the rigorous semi-analytic expression for the  $N$ -channel Jost matrix derived in Ref. 7. In that expression, all the factors responsible for the “bad behavior” of the Jost matrix (i.e., factors depending on the Sommerfeld parameters and the channel momenta responsible for the branching of the Riemann surface) are given explicitly. The remaining unknown factors are analytic and single-valued functions of  $E$  defined on a simple energy plane. These functions are expanded in the Taylor series, and the expansion coefficients serve as the fitting parameters.

## 2. Parametrization

In Ref. 7, it was shown that for a nonrelativistic reaction of the type  $a + b \rightarrow c + d$  involving charged particles, the  $N$ -channel Jost matrix has the following general form:

$$f_{mn}^{(\text{in/out})}(E) = \frac{e^{\pi\eta_m/2}\ell_m!}{2\Gamma(\ell_m + 1 \pm i\eta_m)} \left\{ \frac{C_{\ell_n}(\eta_n)k_n^{\ell_n+1}}{C_{\ell_m}(\eta_m)k_m^{\ell_m+1}} A_{mn}(E) - \left[ \frac{2\eta_m h(\eta_m)}{C_0^2(\eta_m)} \pm i \right] C_{\ell_m}(\eta_m) C_{\ell_n}(\eta_n) k_m^{\ell_m} k_n^{\ell_n+1} B_{mn}(E) \right\}, \quad (1)$$

where

$$k_n = \pm \sqrt{\frac{2\mu_n}{\hbar^2}(E - E_n)}, \quad n = 1, 2, \dots, N, \quad (2)$$

are the channel momenta determined by the differences between the total energy  $E$  and the channel thresholds  $E_n$ , as well as by the corresponding reduced masses  $\mu_n$ ; the channel angular momenta and the Sommerfeld parameters are  $\ell_n$  and  $\eta_n = \mu_n e^2 Z_1 Z_2 / (k_n \hbar^2)$ ; the function

$$C_\ell(\eta) = \frac{2^\ell e^{-\pi\eta/2}}{\Gamma(2\ell + 2)} |\Gamma(\ell + 1 \pm i\eta)| \quad (3)$$

is the Coulomb barrier factor; and

$$h(\eta) = \frac{1}{2} [\psi(i\eta) + \psi(-i\eta)] - \ln \hat{\eta}, \quad \psi(z) = \frac{\Gamma'(z)}{\Gamma(z)}, \quad \hat{\eta} = \frac{\mu e^2 |Z_1 Z_2|}{k \hbar^2}. \quad (4)$$

It is shown that the remaining unknown matrices  $A(E)$  and  $B(E)$  in Eq. (1) are single-valued and analytic functions of the energy, defined on a simple energy plane without branching points. All the complicated topology of the Riemann surface where the Jost functions are defined is determined by the coefficients of the matrices  $A(E)$  and  $B(E)$ , given in Eq. (1) explicitly.

If for a given energy  $E$  the Jost matrices (1) are known, then the corresponding  $S$ -matrix is just their “ratio,”

$$S(E) = f^{(\text{out})}(E) [f^{(\text{in})}(E)]^{-1}, \quad (5)$$

and the scattering cross-section for the channel  $n \rightarrow m$  can be found as

$$\sigma_{mn}(E) = \frac{\pi}{k_n^2} (2\ell_n + 1) |S_{mn}(E) - \delta_{mn}|^2. \quad (6)$$

The resonances are the points

$$\mathcal{E} = E_r - \frac{i}{2}\Gamma, \quad E_r > 0, \quad \Gamma > 0, \quad (7)$$

on the Riemann surface of the energy, where

$$\det f^{(\text{in})}(\mathcal{E}) = 0 \quad (8)$$

and therefore where the  $S$ -matrix has poles.

The energy surface has a square-root branching point at every channel threshold  $E_n$ . This is because the Jost matrices depend on the energy  $E$  via the channel momenta (2) and for each of them there are two possible choices of the sign in front of the square root. The resonance spectral points are located on the so-called nonphysical sheet of this Riemann surface, i.e., such a layer of the surface where all the channel momenta have negative imaginary parts. In the numerical calculations, the choice of the sheet is done by an appropriate choice of the signs in front of the square roots (2).

Since the matrices  $A(E)$  and  $B(E)$  are analytic, they can be expanded in the Taylor series around any complex point  $E_0$ . Near this point, they can therefore be

approximated by the first  $M$  terms of these series:

$$A(E) \approx \sum_{i=0}^M a_i(E_0)(E - E_0)^i, \quad (9)$$

$$B(E) \approx \sum_{i=0}^M b_i(E_0)(E - E_0)^i, \quad (10)$$

where the expansion coefficients  $a_i$  and  $b_i$  are  $(N \times N)$ -matrices. These matrices depend only on the choice of the point  $E_0$ . After finding them, the Jost matrices (1) can be used at any complex energy  $E$  within a circle around  $E_0$ , where the approximations (9, 10) are satisfactory.

We treat the elements of the matrices  $a_i$  and  $b_i$  as the adjustable parameters in the procedure of fitting experimental cross-section. After finding the optimal values for them, we look for the roots of Eq. (8) and thus find the resonance parameters  $E_r$  and  $\Gamma$ . As to the partial widths  $\Gamma_n$ , they can easily be found following the procedure described in Ref. 8. Indeed, we know their sum  $\Gamma = \Gamma_1 + \Gamma_2 + \dots + \Gamma_N$  and we can find their ratios (see Ref. 8):

$$\frac{\Gamma_m}{\Gamma_n} = \lim_{E \rightarrow \mathcal{E}} \left| \frac{S_{mm}(E)}{S_{nn}(E)} \right|. \quad (11)$$

At a resonance energy,  $E = \mathcal{E}$ , all the elements of the  $S$ -matrix are singular because all of them have the same singular factor  $1/\det f^{(\text{in})}(E)$ . However, in the ratio (11) this factor cancels out. Therefore, if we explicitly invert the matrix  $f^{(\text{in})}$  and use it in Eq. (5) without common factor  $1/\det f^{(\text{in})}$ , then we can avoid numerical evaluation of the limit (11). In the simplest case of a two-channel problem, we obtain:

$$\frac{\Gamma_1}{\Gamma_2} = \left| \frac{f_{11}^{(\text{out})} f_{22}^{(\text{in})} - f_{12}^{(\text{out})} f_{21}^{(\text{in})}}{f_{22}^{(\text{out})} f_{11}^{(\text{in})} - f_{21}^{(\text{out})} f_{12}^{(\text{in})}} \right|_{E=\mathcal{E}}, \quad N = 2. \quad (12)$$

It should be noted that such a simple and numerically stable procedure for calculating the partial widths is only possible when the Jost matrices are parametrized. If we were parametrizing the  $S$ -matrix directly, then the limits (11) would have to be calculated numerically as the ratios of singular functions.

### 3. Fitting

We assume that there are sets of experimental data available for at least one channel  $n \rightarrow m$  (or perhaps for several channels), i.e., the cross-sections

$$\sigma_{mn}(E_i^{(mn)}) \pm \delta_i^{(mn)}, \quad i = 1, 2, \dots, N^{(mn)}$$

with the corresponding experimental errors (standard deviations)  $\delta^{(mn)}$ , measured at the collision energies  $E_i^{(mn)}$ . The center  $E_0$  of the expansions (9, 10) can be chosen somewhere within the interval covered by these collision energies (where we

expect to find a resonance). The optimal values of the expansion parameters are found by minimizing the following  $\chi^2$  function

$$\begin{aligned} \chi^2 = & \sum_{i=1}^{N^{(mn)}} \left[ \frac{\sigma_{mn}(E_i^{(mn)}) - \sigma_{mn}^{\text{fit}}(E_i^{(mn)})}{\delta_i^{(mn)}} \right]^2 \\ & + \sum_{j=1}^{N^{(m'n')}} \left[ \frac{\sigma_{m'n'}(E_j^{(m'n')}) - \sigma_{m'n'}^{\text{fit}}(E_j^{(m'n')})}{\delta_j^{(m'n')}} \right]^2 \\ & + \dots + \sum_{m < n, j} |S_{mn}(E_j^{(mn)}) - S_{nm}(E_j^{(mn)})|^2, \end{aligned} \quad (13)$$

where the fitting cross-section  $\sigma_{mn}^{\text{fit}}$  depends on the expansion coefficients via Eqs. (6), (5) and (1). The last sum in the above  $\chi^2$  function makes the fitted  $S$ -matrix symmetric in accordance with the detailed balance theorem (see a more detailed discussion in Ref. 9). The minimization is done using the MINUIT code.<sup>11</sup>

The number of the adjustable parameters depends on the number  $N$  of the existing channels (the data do not have to be available for all of them) and on the number  $M$  of the terms in the Taylor series (9, 10). Generally speaking, the expansion coefficients  $a(E_0)$  and  $b(E_0)$  are the  $N \times N$  matrices of complex elements. However, as was shown in Ref. 7, they become real matrices if the point  $E_0$  is on the real axis. Therefore, if  $E_0$  is on the interval covered by the experimental energies  $E_i^{(mn)}$ , the total number of real fitting parameters is  $2(M + 1)N^2$ .

#### 4. Example

In order to demonstrate the efficiency of the proposed method, we choose a model two-channel problem where the parameters of the resonances can be determined in an exact way. For this model, we generate artificial data points with a typical distribution of errors. In addition to the error-bar for each pseudo-data point, we introduce a random shift (up or down) from the exact cross-section curve, i.e., a typical experimental “noise.” Using these points, we extract the resonance parameters and compare them with the corresponding exact values.

Our artificial data points are generated using the following two-channel potential having a Coulomb tail:

$$V(r) = \begin{pmatrix} -1.0 & -7.5 \\ -7.5 & 7.5 \end{pmatrix} r^2 e^{-r} + \begin{pmatrix} 1 & 0 \\ 0 & 1 \end{pmatrix} \frac{1}{r}. \quad (14)$$

The short-range term in this potential is the same as in the famous Noro–Taylor model.<sup>10</sup> The units in Eq. (14) are therefore the same, namely, they are such that the reduced masses for both channels are equal to one,  $\mu_1 = \mu_2 = 1$ , with  $\hbar c = 1$ , and both angular momenta are zero,  $\ell_1 = \ell_2 = 0$ . The threshold energies for the channels are  $E_1 = 0$  and  $E_2 = 0.1$ .

For a given potential, the matrices  $A(E)$  and  $B(E)$  in Eq. (1) can be found as the solutions of differential equations derived in Ref. 7. This can be done for any complex energy with the help of the complex rotation of the coordinate described in Ref. 8. In this way, we can find the exact Jost matrices and therefore the exact cross-section as well as the exact resonance parameters. The first six resonances thus located for the potential (14) are listed in Table 1.

For each of the elastic channels,  $(1 \rightarrow 1)$  and  $(2 \rightarrow 2)$ , we generated 30 artificial data points in the energy interval  $6 < E < 11$ . In order to make them more realistic, these points were randomly shifted around the corresponding exact cross-section curves, using the Gaussian distribution, i.e., the values  $\sigma_{mn}(E_i^{(mn)})$  were replaced with

$$\sigma_{mn}(E_i^{(mn)}) \rightarrow \sigma_{mn}(E_i^{(mn)})G_i,$$

where  $G_i$  were the normally distributed random numbers with the mean value 1 and the standard deviation  $\Delta$ . We used three values of  $\Delta$ , namely, 0.01, 0.05 and 0.10. This was done to test the stability of the method.

Table 1. The resonance energies and widths generated by the potential (14).

	$E_r$	$\Gamma$	$\Gamma_1$	$\Gamma_2$
1	6.278042551	0.036866729	0.006898807	0.029967922
2	8.038507867	2.563111275	0.617710684	1.945400591
3	8.861433400	7.883809113	1.949506410	5.934302704
4	9.020824224	14.07907263	3.591961102	10.48711153
5	8.566130944	20.75266055	5.414178669	15.33848188
6	7.548492959	27.69926473	7.328979882	20.37028485

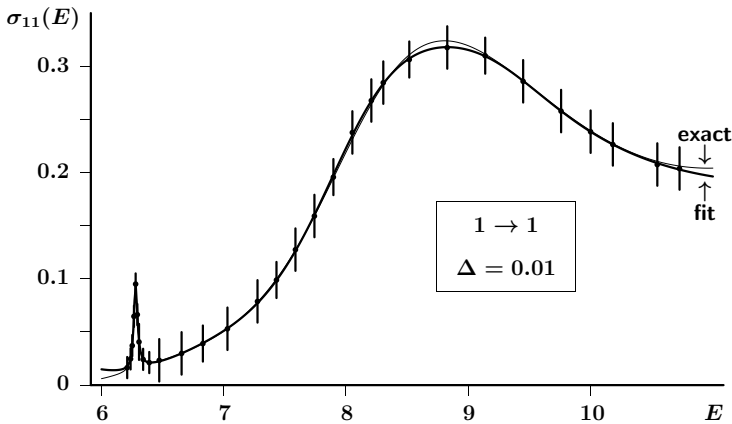


Fig. 1. The data points for the elastic channel  $(1 \rightarrow 1)$  together with the curves showing the exact and fitted cross-sections. The experimental noise for the points has the normal distribution with the standard deviation  $\Delta = 0.01$ .

The center of expansion was taken as  $E_0 = 8$ . In the case of low experimental noise ( $\Delta = 0.01$ ), we used  $M = 5$ , i.e., the first six terms of the series (9, 10) were taken into account. For higher noise, the number of terms in the expansions was smaller, namely,  $M = 3$ . The reason for such a choice was that with larger  $M$ , the fitting curve tries to pass through almost all the data points and thus does noisy zigzags, which result in a loss of overall accuracy.

Figure 1 shows the exact cross-section  $\sigma_{11}(E)$ , the artificial data points with  $\Delta = 0.01$ , and the curve obtained by fitting these points. The same information for the channel ( $2 \rightarrow 2$ ) is given in Fig. 2 (also for  $\Delta = 0.01$ ). Similarly, Figs. 3–6 show the corresponding exact and fitted cross-sections as well as the data points for stronger experimental noise, namely, for  $\Delta = 0.05$  and  $\Delta = 0.10$ .

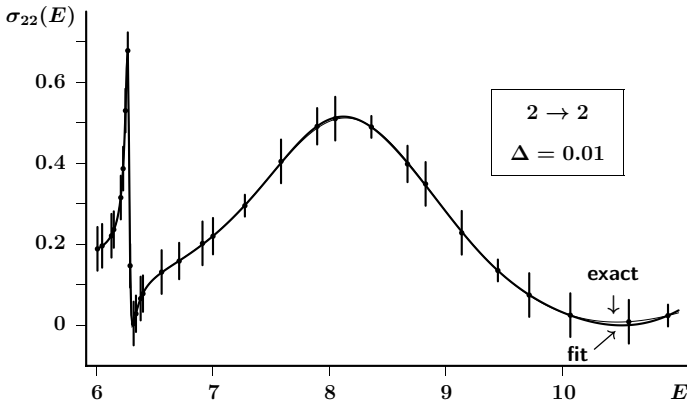


Fig. 2. The data points for the elastic channel ( $2 \rightarrow 2$ ) together with the curves showing the exact and fitted cross-sections. The experimental noise for the points has the normal distribution with the standard deviation  $\Delta = 0.01$ .

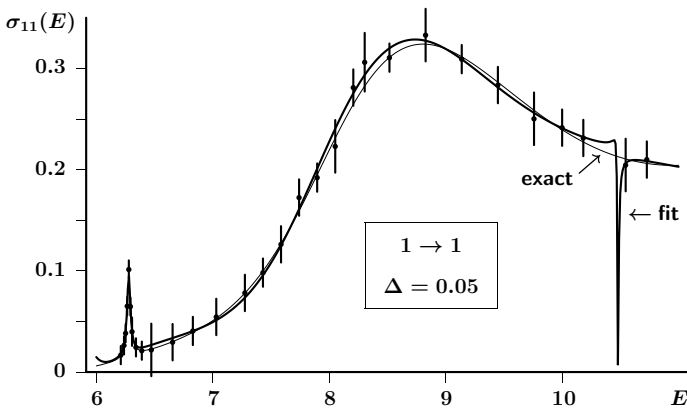


Fig. 3. The data points for the elastic channel ( $1 \rightarrow 1$ ) together with the curves showing the exact and fitted cross-sections. The experimental noise for the points has the normal distribution with the standard deviation  $\Delta = 0.05$ .

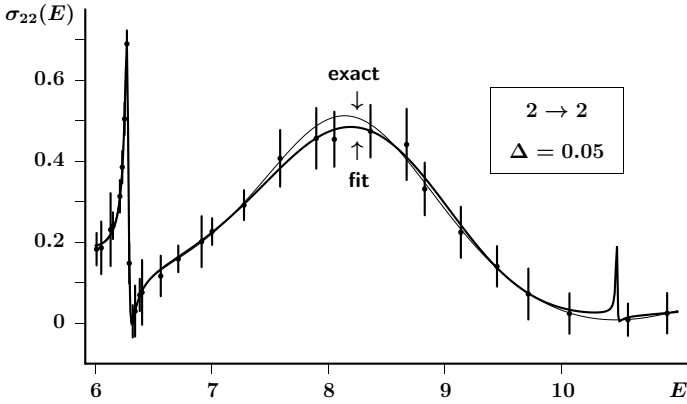


Fig. 4. The data points for the elastic channel ( $2 \rightarrow 2$ ) together with the curves showing the exact and fitted cross-sections. The experimental noise for the points has the normal distribution with the standard deviation  $\Delta = 0.05$ .

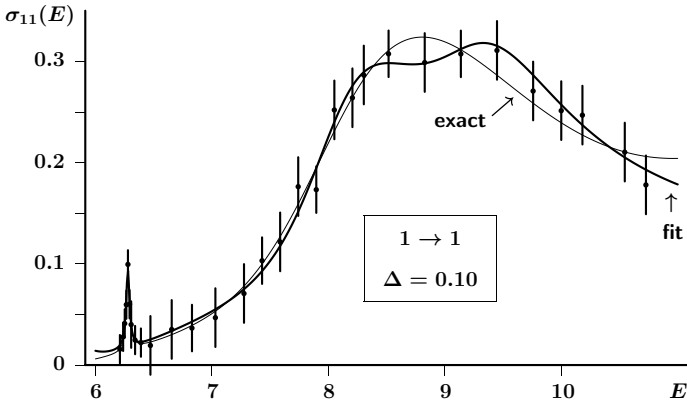


Fig. 5. The data points for the elastic channel ( $1 \rightarrow 1$ ) together with the curves showing the exact and fitted cross-sections. The experimental noise for the points has the normal distribution with the standard deviation  $\Delta = 0.10$ .

In fitting the data points in the elastic channels ( $1 \rightarrow 1$ ) and ( $2 \rightarrow 2$ ) all matrix elements of the Jost matrices are involved. As a result, not only the diagonal but also the off-diagonal elements of the  $S$ -matrix should be close to the correct values. This means that even without having any data points in the inelastic channels, we should obtain the cross-sections  $\sigma_{21}(E)$  and  $\sigma_{12}(E)$  that are not far from the corresponding exact curves. Figure 7 shows the exact cross-section for the inelastic channel ( $1 \rightarrow 2$ ) and the curves obtained for it with  $\Delta = 0.01$ ,  $0.05$ , and  $0.10$ . Of course, as one would expect, the greater the accuracy of the experimental data, the more accurate is the prediction for the cross-section in the channel where no data are available.

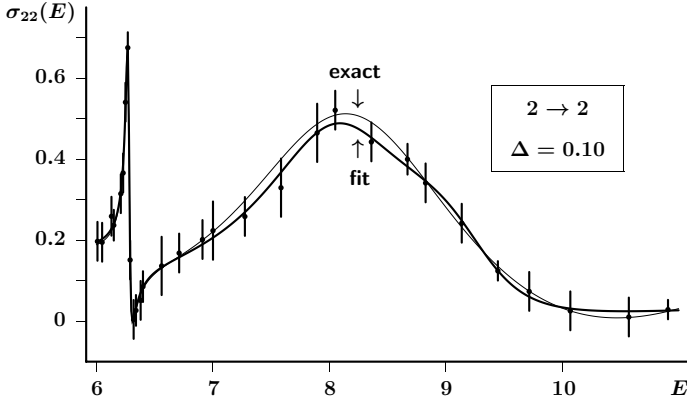


Fig. 6. The data points for the elastic channel ( $2 \rightarrow 2$ ) together with the curves showing the exact and fitted cross-sections. The experimental noise for the points has the normal distribution with the standard deviation  $\Delta = 0.10$ .

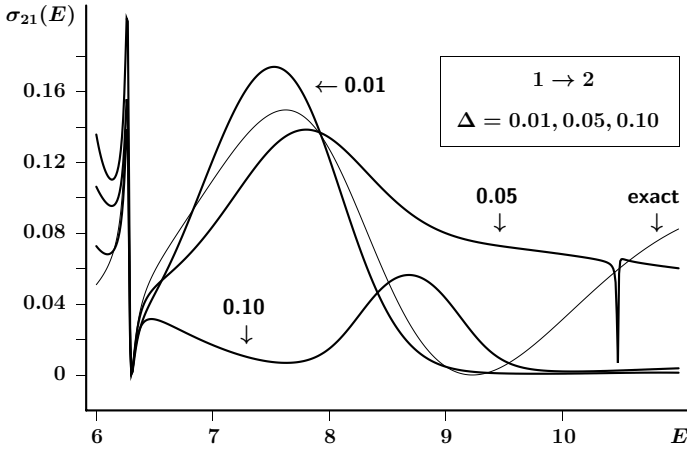


Fig. 7. Exact inelastic cross-section (thin curve) for the channel ( $1 \rightarrow 2$ ) and the approximate curves obtained after fitting the data in the elastic channels with the experimental noise determined by the standard deviations  $\Delta = 0.01, 0.05, \text{ and } 0.10$ .

After fitting the data, we looked for the roots of Eq. (8) on the nonphysical sheet of the Riemann surface of the energy. For this sheet, the signs in Eq. (2) are chosen in such a way that both channel momenta  $k_1$  and  $k_2$  have negative imaginary parts. The roots thus found correspond to the resonance spectral points. They are listed in Table 2 for all three levels of the experimental noise. Of course, the more accurate the measurements, the closer to the exact values are the extracted resonance parameters. Even with very high experimental noise ( $\Delta = 0.10$ ) we are still able to extract at least the first resonance with a reasonable accuracy.

Table 2. The resonance parameters obtained from fitting the data with different degrees of experimental noise.

Resonance	$\Delta$	$E_r$	$\Gamma$	$\Gamma_1$	$\Gamma_2$
1	exact	6.278042552	0.036866729	0.006898807	0.029967922
	0.01	6.277997424	0.036731019	0.006721542	0.030009477
	0.05	6.278563562	0.035568397	0.006497720	0.029070677
	0.10	6.278669302	0.036236713	0.006638945	0.029597768
2	exact	8.038507867	2.563111275	0.617710684	1.945400591
	0.01	7.998939904	2.096675299	0.623726003	1.472949296
	0.05	7.676616089	2.502856671	0.792088450	1.710768220
	0.10	7.968634195	1.662113407	0.231505793	1.430607614
3	exact	8.861433400	7.883809114	1.949506410	5.934302704
	0.01	11.21325906	3.204531546	0.031776330	3.172755216
	0.05	9.188805831	2.549030291	0.364986606	2.184043685
	0.10	9.259323135	2.226793463	1.232709401	0.994084062

## 5. Conclusion

The main idea of the proposed method has its roots in the so-called “effective-range expansion” widely used in nuclear and atomic physics (see, for example, Ref. 1). Within this approach, a certain function of the scattering phase-shift is expanded in the power series of the collision energy, and the expansion coefficients are used as the adjustable parameters to fit experimental data. Traditional effective-range expansion is very useful but is limited to low energies. Moreover, it is difficult to apply it to multi-channel processes.

We generalize this approach and thus remove all these limitations. First of all, we expand a more fundamental quantity: the Jost matrix. When the Jost-matrix expansion in the power series is obtained, one can easily derive the corresponding expansion of the  $S$ -matrix, the phase-shift, or any other quantity that is needed. Secondly, it is not necessary to do the expansion near the point  $E = 0$ . Actually, the expansion can be done around any complex value of variable  $E$ . Concerning the multi-channel problems, for the Jost matrices, this does not pose any difficulty. Simply, the expansion coefficients become matrices.

In order to expand a function in the Taylor series of  $E$ , one has to be sure that this function is an analytic and single-valued function of  $E$ . However, all the quantities describing the scattering processes (amplitude,  $S$ -matrix, Jost matrix, etc) are multi-valued functions defined on a complicated Riemann surface of the energy with the number of branch points equal to the number of channels. In order to circumvent this difficulty, we use earlier derived general semi-analytic expression for a multi-channel Jost matrix, where all the factors responsible for its “bad behavior,” are given explicitly. The remaining unknown functions are more simple, more smooth, and (more importantly) are analytic and single-valued functions defined on a simple energy plane. We only do the expansion for these functions.

In our earlier publication,<sup>9</sup> we demonstrated how the proposed method works for the reactions involving neutral particles. In the present paper, we consider a more

general case when the potential has both a short-range part and a Coulomb tail. Similar to the simple effective-range theory, the presence of the Coulomb potential makes the explicit coefficients in the semi-analytic expression for the Jost matrix more complicated. However, the remaining functions of  $E$  are still smooth and can be approximated by just a few terms of the Taylor series. We have demonstrated this using a two-channel model.

We have shown that even with rather inaccurate experimental data ( $\Delta = 0.10$  in our model) the resonances can still be found. For the narrow resonance, we managed to reproduce not only the energy and total width, but the partial widths as well, when the data points had rather big deviations from the exact values. For a wide resonance (the resonance number 2) with such a high experimental noise, we still obtained reasonable parameters. And even the energy of the extremely wide resonance (number 3) was obtained, not far from the exact value. This shows that the proposed method is accurate and stable.

One of the advantages of the proposed method is that the fitting procedure involves all matrix elements of the Jost matrix and therefore all elements of the  $S$ -matrix even if the data are available just in one channel. The resulting  $S$ -matrix should therefore be correct in all channels. This means that by fitting accurately-measured data in one or two channels, we could in principle obtain a reasonable estimate for the cross-section in the other channels where the measurements are difficult or impossible.

It should be noted that the proposed method is nonrelativistic and therefore cannot be directly used in high-energy physics. There are however a wide range of problems in atomic and low-energy nuclear physics, where it could find applications. In principle, one can try the same parametrization for high energies as well, if the relativistic relation between the energy and momentum,  $E = \sqrt{\hbar^2 k^2 c^2 + \mu^2 c^4}$ , is used in all the formulae. Such “intuitive” inclusion of relativistic kinematics into nonrelativistic operators is very common for various parametrizations of scattering data in particle physics. In our case, however, this would mean that mathematical rigor and substantiation are lost.

## References

1. V. I. Kukulin, V. M. Krasnopolsky and J. Horáček, *Theory of Resonances* (Kluwer Academic Publishers, Dordrecht/Boston/London, 1989), pp. 276–295.
2. Nstar 2005, *Proceedings of the Workshop on the Physics of Excited Nucleons*, Florida State University, Tallahassee, USA (12–15 October 2005), World Scientific (2006), pp. 1–66.
3. G. Breit and E. Wigner, *Phys. Rev.* **49** (1936) 519.
4. S. A. Rakityansky, S. A. Sofianos and N. Elander, *J. Phys. A: Math. Theor.* **40** (2007) 14857.
5. P. Masjuan and J. J. Sanz-Cillero, *Eur. Phys. J. C* **73** (2013) 2594.
6. A. Švarc, M. Hadžimehmedović, H. Osmanović, J. Stahov, L. Tiator and L. R. Workman, *Phys. Rev. C* **88** (2013) 035206.
7. S. A. Rakityansky and N. Elander, *J. Math. Phys.* **54** (2013) 122112.

8. S. A. Rakityansky and N. Elander, *Int. J. Quantum Chem.* **109** (2006) 1105.
9. S. A. Rakityansky and N. Elander, *Int. J. Mod. Phys. E* **22** (2013) 1350032.
10. T. Noro and H. S. Taylor, *J. Phys. B: Atom. Mol. Phys.* **13** (1980) L377.
11. F. James and M. Roos, *Comp. Phys. Comm.* **10** (1975) 343, <http://hep.fi.infn.it/minuit.pdf>.